

**Electronic signature of MnAs phases
in bare and buried films grown on GaAs(001)**

M. Moreno^{a)}

Instituto de Ciencia de Materiales de Madrid (CSIC), Cantoblanco, 28049 Madrid, Spain

A. Kumar,^{*} M. Tallarida,^{b)}

Fritz-Haber-Institut der Max-Planck-Gesellschaft, Faradayweg 4-6, 14195 Berlin, Germany

A. Ney,^{c)} K. H. Ploog

Paul-Drude-Institut für Festkörperelektronik, Hausvogteiplatz 5-7, 10117 Berlin, Germany

K. Horn

Fritz-Haber-Institut der Max-Planck-Gesellschaft, Faradayweg 4-6, 14195 Berlin, Germany

(Date: 16 June 2008)

Photoelectron emission (PES) analyses of the arsenic bonding in the near-surface region of an initially arsenic capped MnAs(1100) film grown on GaAs(001) have been carried out for progressive thermal decapping stages. Electronically distinct As-bonding states are identified, that we assign to bulk MnAs phases, bulk arsenic, and interfacial environments. The arsenic coating imposes mechanical constraints to the MnAs film, in addition to those imposed by the GaAs substrate, which appear to alter the relative stability of the α and β MnAs phases around room temperature.

^{a)} Electronic mail: mmoreno@icmm.csic.es

^{b)} Present address: BTU Cottbus, Angewandte Physik und Sensorik, Konrad-Wachsmann-Allee 17, 03046 Cottbus, Germany

^{c)} Present address: Experimentalphysik, Universität Duisburg-Essen, Lotharstrasse 1, D-47057 Duisburg, Germany

I. Introduction

α -MnAs is a ferromagnetic metal, candidate to be part of semiconductor-based spintronic and magnetologic devices.¹⁻³ With this underlying interest, high-quality epitaxial MnAs films have been successfully grown on several GaAs substrate orientations.^{1,4} However, these films exhibit peculiar magneto-structural properties, as compared to bulk MnAs. In bulk MnAs, the non-ferromagnetic orthorhombic β -MnAs phase abruptly transforms at $\sim 40^\circ\text{C}$ into the ferromagnetic hexagonal α -MnAs phase. However, in MnAs films grown on GaAs(001) and GaAs(111)B substrates, the α and β phases coexist within a relatively wide temperature range (~ 10 - 50°C).^{4,5} The phase coexistence mechanism has a major impact on the properties of MnAs films, limiting their performance as a ferromagnetic material. Optimal performance would be achieved if the ferromagnetic α -MnAs phase could be stabilized (at room temperature) against transformation into non-ferromagnetic β -MnAs phase. In this paper, we examine the arsenic bonding configurations in bare and arsenic-coated MnAs(1100) films grown on GaAs(001), using photoelectron emission spectroscopy. Hence we get insight into how arsenic coating alters the relative stability of the α and β MnAs phases.

II. Experiment

A 120 nm-thick MnAs film was grown on a heavily n-type doped GaAs (001) $\pm 0.5^\circ$ epi-ready substrate by MBE. Prior to MnAs growth, a GaAs buffer layer was grown at high temperature (550-600 $^\circ\text{C}$) following standard procedures. MnAs growth was initiated on a carefully prepared As-rich $d(4\times 4)$ or $c(4\times 4)$ GaAs template, and proceeded at a substrate temperature of 230 $^\circ\text{C}$, with a growth rate of 19 nm/h, and an As₄-to-Mn beam-equivalent-

pressure (BEP) ratio of 49. Under these growth conditions, MnAs films are known to have the so-called “A” epitaxial orientation,⁴ with MnAs(1100) parallel to GaAs(001). After MnAs growth, the sample was annealed at 286°C for 12 min. Then, the sample was cooled down well below room temperature and was exposed to As₄ flux in order to deposit a protective arsenic coating. Before the photoemission analysis, the sample was stored under vacuum and only shortly exposed to air during the time necessary to cut it into pieces and to transfer it from the growth to the analysis chamber. Photoemission analyses were carried out in an experimental station connected to the UE56/2-PGM-2 beamline of the BESSY II synchrotron-radiation facility. The arsenic-coated sample was mounted on a variable-temperature holder, using Ga-In eutectic alloy as glue on the back side of the sample. The arsenic coating was progressively desorbed by heating the sample up to increasing temperatures (three heating steps) in the range ~300-370°C. Photoemission spectra were recorded at room temperature after each decapping step. Photoemitted electrons were collected in the direction normal to the sample surface in an angle-integrated mode using an ESCALAB MkII electron energy analyzer. The binding energy scale of the spectra shown below refers to the Fermi energy. Line-shape analyses were performed with the aid of the CasaXPS software.

III. Results and discussion

Figure 1 shows overview photoemission spectra recorded on the unheated (arsenic-coated) sample and for progressive arsenic-decapping stages (1 to 3). For the unheated sample, the most prominent features are arsenic core-level signals, as well as associated plasmon losses. No Mn-related features are seen, indicating that the MnAs layer is well covered by the

arsenic coating. After the first decapping step, Mn-related features show up. Most of the initial arsenic coating has been desorbed, although residual pure arsenic appears to remain on top of the MnAs layer. The decapping steps 2 and 3 progressively remove the residual top arsenic. Spectrum “3” exhibits prominent Mn 3*p* and Mn Auger signals. No energy shifts are observed for Mn core-level signals corresponding to the arsenic-decapping steps 1 to 3. After the third decapping step, the arsenic coating appears effectively removed, and bare stoichiometric MnAs exposed.

Dramatic changes in the As 3*d* photoemission spectral shape are observed upon thermally desorbing the residual top arsenic (see Fig. 2). To understand the changes, we calculated theoretical As 3*d* envelope curves (shown in Fig. 3) by adding up spin-orbit split doublets [characterized by 3*d*_{5/2} binding energy, asymmetry, and full-width at half-maximum (FWHM) values], corresponding to specific As-bonding configurations.⁶ For all of the doublets considered, the spin-orbit splitting was fixed to 0.68 eV, and the branching ratio (area ratio) was fixed to the theoretical 2:3 value. The parameters of the spectral components for each decapping stage are listed in Table I. The As 3*d* spectrum recorded after the first decapping step (curve “1” in Fig. 3) is fitted by three components: A, α , and I. On the other hand, the spectrum recorded after the third decapping step (curve “3” in Fig. 3) is fitted by two narrow-width components, α and β , and an additional broad component, D. The As 3*d* spectrum recorded after the second decapping step (curve “2” in Fig. 3) requires at least four components to reach a good fit: A, β , α_1 , and α_2 . The α component drawn for spectrum “2” in Fig. 3 was constructed by adding up the α_1 and α_2 doublets. This α component (BE=40.63 eV) is centered at roughly the same binding energy as for spectra “1” and “3”. There is no contribution of type-A component for stage “3”, and a small contribution for stage “2”. The “A” component is obviously associated to the arsenic coating (arsenic in a bulk As

environment), which desorbs upon heating. We assign the “ α ” component to arsenic in a bulk MnAs environment and the “I” component (spectrum “1”) to arsenic at the As/MnAs interface. The “D” component (spectrum “3”) accounts for electronically disordered environments, present in bare MnAs. We next discuss the origin of the “ β ” component in the context of previous reports and considering additional experimental data for bare MnAs (stage “3”).

Okabayashi et al. and Ouerghi et al. previously reported photoemission results for bare MnAs films grown on GaAs.^{7,8} The As 3*d* spectrum reported⁷ by Okabayashi et al. for a thick MnAs film grown on GaAs(001) much resembles the As 3*d* spectrum reported⁸ by Ouerghi et al. for a (3x1)-reconstructed MnAs film grown on GaAs(111)B, and it is similar to the As 3*d* spectrum reported here for arsenic-decapped bare MnAs grown on GaAs(001) [curve “3” in Fig. 3]. The common feature of these spectra is the pronounced shoulder/peak on the low binding energy side, which indicates that the line-shape is contributed by at least two intense doublets. Both Okabayashi’s and Ouerghi’s groups invoked interpretations of the As 3*d* spectral shape for bare MnAs films grown on GaAs(001) and GaAs(111)B substrates, respectively, in terms of a single “bulk” component and additional “surface” components. However, despite the line-shape similarity, they did not agree on where to locate the “bulk” component, which should be equivalent for both experiments: whereas Ouerghi et al. interpreted the low binding energy component as a “bulk” component, Okabayashi et al. interpreted it as a “surface” component.

The existence of local surface reconstructions on epitaxial MnAs films is well documented.^{9,10} However, this does not guarantee that a split surface component must be observable in core-level photoemission spectra. The energy splitting and intensity of the

surface component may not be large enough to allow clear distinction, and the surface component may be obscured by other dominating chemically shifted components. We note that local surface reconstructions have been also observed for epitaxial MnSb films (Ref. ¹¹), but Sb 4*d* spectra recorded on such films (Ref. ¹²) are simple, being well fitted by a single doublet. That is, the PES spectral shape of anion core levels is essentially different for MnAs and for MnSb films at room temperature. The similarity of the As 3*d* spectral features observed for bare MnAs films with different epitaxial orientations [grown on GaAs(001) and GaAs(111)B substrates] and subjected to different surface treatments (as-grown versus arsenic-decapped films) points towards a bulk (rather than surface) origin of these spectral features. The main As 3*d* spectral features for bare MnAs films at RT (curve 3 in Fig. 3) appear better interpreted as all bulk components. We assume that the low binding energy β component, centered at 40.14 eV, and the α component, centered at \sim 40.64 eV, are both bulk components and assign them to the β -MnAs and α -MnAs phases, respectively. Within this interpretation, the peculiar As 3*d* line-shape observed for bare MnAs films at RT is reflecting the α - β phase coexistence.

The As 3*d* spectra shown in Figs. 4 and 5 provide further support to the interpretation in terms of separated α -MnAs and β -MnAs contributions. These spectra have been recorded at RT on the bare MnAs film (stage “3”) following two different temperature pathways: reaching room temperature from high and low temperature, respectively. Thermal hysteresis is observed: the photoemission signal in the low binding energy side of the spectra (Fig. 4) is seen to be weaker for the spectrum recorded following a low-temperature pathway (heating up to RT) than for the spectrum recorded following a high-temperature pathway (cooling down to RT). The relative intensities/amounts of the α and β components/phases, as well as of disorder (D component), derived from the As 3*d* line-shape analyses for the two pathways

(Fig. 5), are listed in Table II. Within an interpretation in terms of a single “bulk” component and additional “surface” components, there should be no thermal hysteresis. Therefore, the results of Figs. 4 and 5 do not support such interpretation. On the other hand, non-relaxed MnAs films on GaAs(001) are known to exhibit pronounced thermal hysteresis in the α/β phase ratio around room temperature.⁴ Such that the results of Figs. 4 and 5 are consistent with an interpretation in terms of α -MnAs and β -MnAs related components. We do not expect the MnAs film studied to have relaxed during the annealing steps performed for arsenic decapping. They were carried out at mild temperatures (300-370°C) and relaxation of such thick MnAs films reportedly require higher temperature (600°C).¹³

The α -MnAs phase appears thus stable in arsenic-covered MnAs, constrained by bottom GaAs and top As (curve “1” in Fig. 3). On the other hand, the α -MnAs and β -MnAs phases coexist in bare MnAs, with no top constrain (curve “3” in Fig. 3). At stage “2”, the sample seems to be covered by arsenic in some regions (there is a small “A” contribution) and to expose bare MnAs in other regions (there is a small “ β ” contribution). Such a situation implies laterally changing mechanical constrains imposed from top to the MnAs film. Hence, the spreading in binding energy of the α component for stage “2” might correlate to laterally varying structural distortions in the α -MnAs phase of the film.

IV. Summary

The arsenic bonding in the near-surface region of an initially arsenic-capped MnAs(1100) film grown on GaAs(001) has been analyzed, for progressive decapping stages, by photoelectron emission spectroscopy. In As 3*d* spectra recorded on bare MnAs, we have

identified two electronically distinct components, α and β , that we assign to arsenic in α -MnAs and β -MnAs environments, respectively. The β component has been found to be absent for MnAs covered by a thin As layer. We conclude that different strain-minimization mechanisms are operative in bare and arsenic-coated MnAs films: the additional mechanical constrain imposed to the MnAs film by the arsenic coating appears to result in stabilization of the ferromagnetic α -MnAs phase against transformation into non-ferromagnetic β -MnAs around room temperature.

Acknowledgments

We thank the BESSY staff for support. This work has been supported by the Spanish Ministry of Education and Science (“Ramón y Cajal” and “Materials” Programs, 2005 call and MAT2004-05348 grant, respectively) and by the German Federal Ministry for Education and Research.

Figure captions

Figure 1. Overview photoemission spectra recorded with 750 eV photons on an initially arsenic-capped MnAs thick film grown on GaAs(001): before heating, on the arsenic-coated sample (bottom spectrum), and for progressive thermal decapping stages “1” to “3” (top spectra). Spectra are shown after subtraction of a Tougaard-type background and normalized to the area of the As 3*p* peak.

Figure 2. High-resolution As 3*d* photoemission spectra recorded with 154 eV photons for the decapping stages: 1 (open square symbols), 2 (open diamond symbols), and 3 (solid circles), after background subtraction and normalization to the peak area.

Figure 3. Line-shape analyses of the As 3*d* photoemission spectra shown in Fig. 2, for the decapping stages “1” to “3”. Theoretical envelope curves are shown superimposed to the experimental data. For stage 2, the α component has been constructed by adding up the α_1 and α_2 subcomponents.

Figure 4. As 3*d* photoemission spectra recorded with 154 eV photons on bare MnAs (stage “3”) at room temperature, following two different thermal pathways: (i) cooling the sample from high ($T > 60^\circ\text{C}$) temperature (solid symbols) and (ii) heating the sample from low ($T < 0^\circ\text{C}$) temperature (open symbols).

Figure 5. Line-shape analyses of the As 3*d* photoemission spectra shown in Fig. 4, corresponding to different thermal pathways.

Table captions

Table I. Binding energy, asymmetry parameter, and full-width at half-maximum (FWHM) for the spectral components considered in the line-shape analyses of Fig. 3, corresponding to progressive decapping stages (1 to 3) of an initially As-coated MnAs film grown on GaAs(001). Binding energies refer to the $5/2$ spin-orbit split $3d$ component. They are expressed relative to the Fermi level.

Table II. Relative intensity of the different components (α , β , D) contributing to the As $3d$ photoemission spectra shown in Fig. 5, recorded on bare MnAs (stage “3”) at room temperature following two different pathways: (i) cooling the sample from high ($T > 60^\circ\text{C}$) down to room temperature and (ii) heating the sample from low ($T < 0^\circ\text{C}$) up to room temperature.

References

- * This paper is dedicated to the memory of Ashwani Kumar whose tragic death in a traffic accident occurred on May 17th.
- ¹ M. Tanaka, *Semicond. Sci. Technol.* **17**, 327 (2002).
- ² C. Pampuch, A. K. Das, A. Ney, L. Däweritz, R. Koch, and K. H. Ploog, *Phys. Rev. Lett.* **91**, 147203 (2003).
- ³ D. Saha, M. Holub, P. Bhattacharya, and Y. C. Liao, *Appl. Phys. Lett.* **89**, 142504 (2006).
- ⁴ L. Däweritz, *Rep. Prog. Phys.* **69**, 2581 (2006).
- ⁵ V. M. Kaganer, B. Jenichen, F. Schippan, W. Braun, L. Däweritz, and K. H. Ploog, *Phys. Rev. Lett.* **85**, 341 (2000).
- ⁶ To simulate asymmetric photoemission peaks, related to metallic electronic configurations, we used DS(γ ,499) line shapes (CasaXPS notation), which stand for Doniach-Sunjić profiles with asymmetry parameter γ , numerically convoluted with a Gaussian described by 499 digital nodes. To simulate symmetric photoemission peaks, we used GL(30) line shapes, which stand for Gaussian/Lorentzian product formulas with 30% of Lorentzian weight, which approximate Voigt-type profiles.
- ⁷ J. Okabayashi, K. Kanai, K. Kubo, S. Toyoda, M. Oshima, K. Ono, and J. Yoshino, *Appl. Phys. Lett.* **89**, 022502 (2006).
- ⁸ A. Ouerghi, M. Marangolo, M. Eddrief, B. B. Lipinski, V. H. Etgens, M. Lazzeri, H. Cruguel, F. Sirotti, A. Coati, and Y. Garreau, *Phys. Rev. B* **74**, 155412 (2006).
- ⁹ M. Kästner, F. Schippan, P. Schützendübe, L. Däweritz, and K. Ploog, *J. Vac. Sci. Technol. B* **18**, 2052 (2000).
- ¹⁰ A. Ouerghi, M. Marangolo, M. Eddrief, S. Guyard, V. H. Etgens, and Y. Garreau, *Phys. Rev. B* **68**, 115309 (2003).

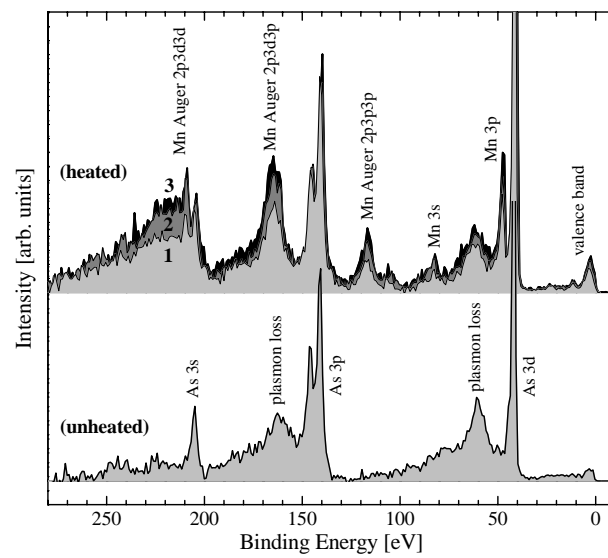
- ¹¹ S. A. Hatfield and G. R. Bell, Surf. Sci. **601**, 5368 (2007).
- ¹² K. Ono, M. Shuzo, M. Oshima, and H. Akinaga, Phys. Rev. B **64**, 085328 (2001).
- ¹³ J. H. Song, Y. Cui, J. J. Lee, and J. B. Ketterson, Appl. Phys. Lett. **87**, 092504 (2005).

Table I

	Componet	Binding Energy [eV]	Asymmetry	FWHM [eV]
Decapping Stage 1	A	41.31	0.10	0.40
	α	40.65	0.13	0.34
	I	40.93	0.13	0.35
Decapping Stage 2	A	41.31	0.12	0.34
	β	40.14	-	0.47
	$\alpha 1$	40.52	0.18	0.41
	$\alpha 2$	40.83	0.18	0.41
Decapping Stage 3	α	40.63	0.18	0.54
	β	40.14	-	0.39
	D	40.67	-	1.15

Table II

	α	β	D
Cooling	57%	20%	23%
Heating	68%	9%	23%



**Fig. 1 - J. Vac. Sci. Technol. B
Moreno et al. - June, 2008**

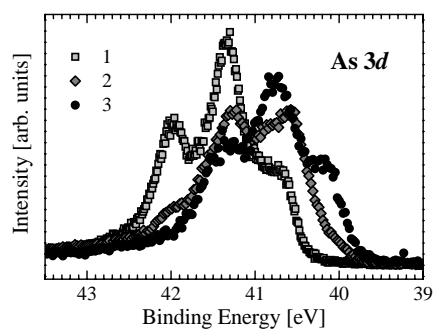


Fig. 2 - J. Vac. Sci. Technol. B
Moreno et al. - June, 2008

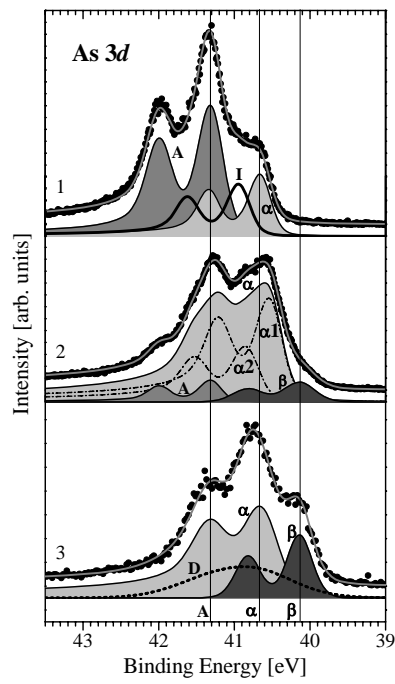
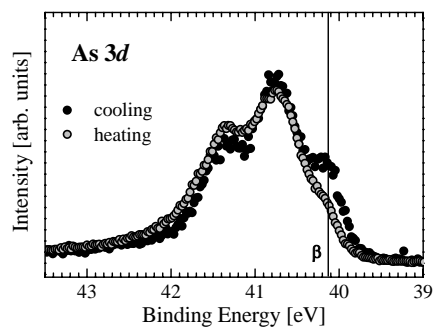


Fig. 3 - J. Vac. Sci. Technol. B
Moreno et al. - June, 2008



**Fig. 4 - J. Vac. Sci. Technol. B
Moreno et al. - June, 2008**

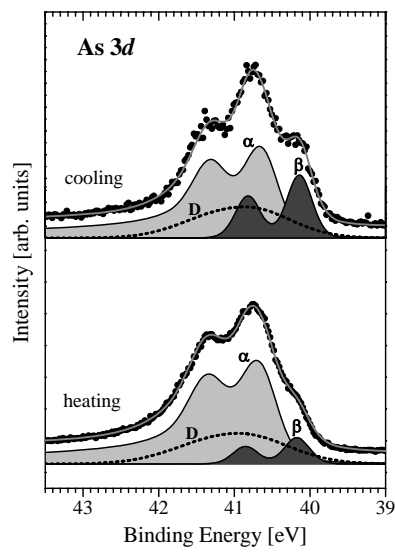


Fig. 5 - J. Vac. Sci. Technol. B
Moreno et al. - June, 2008